Journal of Engineering Mathematics **42:** 291–301, 2002.

Generalised critical free-surface flows

F. DIAS[A] and J.-M. VANDEN-BROECK[B]
[a]*Centre de Mathématiques et de Leurs Applications, Ecole Normale Supérieure de Cachan, 61 avenue du Président Wilson, 94235 Cachan cedex, France*
[b]*School of Mathematics, University of East Anglia, Norwich NR4 7TJ, UK*

Received 1 October 2001; accepted in revised form 8 December 2001

Abstract. Nonlinear waves in a forced channel flow are considered. The forcing is due to a bottom obstruction. The study is restricted to steady flows. A weakly nonlinear analysis shows that for a given obstruction, there are two important values of the Froude number, which is the ratio of the upstream uniform velocity to the critical speed of shallow water waves, $F_C > 1$ and $F_L < 1$ such that: (i) when $F < F_L$, there is a unique downstream cnoidal wave matched with the upstream (subcritical) uniform flow; (ii) when $F = F_L$, the period of the cnoidal wave extends to infinity and the solution becomes a hydraulic fall (conjugate flow solution) – the flow is subcritical upstream and supercritical downstream; (iii) when $F > F_C$, there are two symmetric solitary waves sustained over the site of forcing, and at $F = F_C$ the two solitary waves merge into one; (iv) when $F > F_C$, there is also a one-parameter family of solutions matching the upstream (supercritical) uniform flow with a cnoidal wave downstream; (v) for a particular value of $F > F_C$, the downstream wave can be eliminated and the solution becomes a reversed hydraulic fall (it is the same as solution (ii), except that the flow is reversed!). Flows of type (iv), including the hydraulic fall (v) as a special case, are computed here using the full Euler equations. The problem is solved numerically by a boundary-integral-equation method due to Forbes and Schwartz. It is confirmed that there is a three-parameter family of solutions with a train of waves downstream. The three parameters can be chosen as the Froude number, the obstruction size and the wavelength of the downstream waves. This three-parameter family differs from the classical two-parameter family of subcritical flows (i) but includes as a particular case the hydraulic falls (ii) or equivalently (v) computed by Forbes.

Key words: boundary-integral method, hydraulic fall, Korteweg–de Vries, potential flow, water waves.

1. Introduction

The theory of free-surface potential flows past submerged obstacles is a classical subject of fluid mechanics. Linearised solutions can be found in Lamb [1, Chapter 9]. Accurate nonlinear solutions were obtained numerically by Forbes and Schwartz [2], Vanden-Broeck [3], Forbes [4], Dias and Vanden-Broeck [5] and others. It is known that there are both steady and unsteady solutions. Here we restrict our attention to steady solutions (the reader who is interested in unsteady solutions is referred to Grimshaw and Smyth [6], Milewski and Vanden-Broeck [7] and to the references cited in those papers).

Following Forbes and Schwartz [2] and Forbes [4], we choose the obstacle to be a semicircular cylinder. Results similar to those presented can be obtained with different obstacle shapes.

The velocity and the height of the uniform flow far upstream are denoted by U and H, respectively. The Froude number upstream is defined by

$$F = \frac{U}{\sqrt{gH}}, \tag{1.1}$$

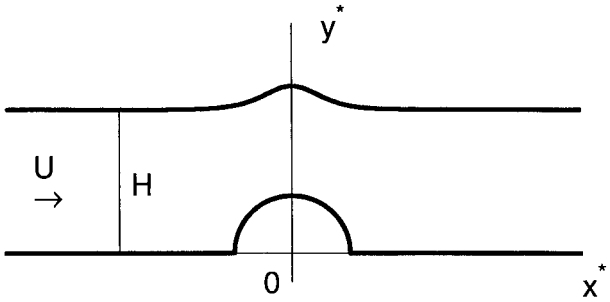

Figure 1. Sketch of the flow. A uniform flow of velocity U and height H approaches a semi-circular obstruction. The radius of the circular bump is R.

where g is the acceleration due to gravity. If $F < 1$, the flow is subcritical. If $F > 1$, the flow is supercritical. If $F > 1$ on one side and $F < 1$ on the other side, the flow is critical. The terms critical, subcritical and supercritical come from linear theory.

Three classes of steady solutions have been computed so far. The first class (i) is subcritical. It is a two-parameter family of solutions in which the flow contains a train of waves downstream and is uniform upstream. The second class (ii) is critical. It is a one-parameter family of waveless solutions. The profiles are non symmetric and the flow is subcritical on one side and supercritical on the other. The third class (iii) is supercritical. It is a two-parameter family of solutions. The profiles are symmetric and waveless in the far field. The results of Vanden-Broeck [3] show that the subcritical class (i) and the supercritical class (iii) are disconnected in the sense that there is an interval of values of the Froude number in which both types of solutions fail to exist.

In this paper we concentrate on supercritical solutions which are wavy downstream (type (iv) of the abstract). A limiting case is the hydraulic fall, in which the waves downstream disappear. Hydraulic falls were observed experimentally and computed numerically by Forbes [4] (for a circular object) and computed numerically by Dias and Vanden-Broeck [5] (for a triangular object). We generalise these findings and demonstrate numerically that there is a three-parameter family of supercritical flows with waves downstream.

2. Formulation

The formulation of the problem follows closely that of Dias and Vanden-Broeck [5] and Forbes and Schwartz [2]. The steady irrotational flow of an incompressible inviscid fluid past a submerged obstruction is considered (see Figure 1). The x^*-axis is chosen to be along the bottom of the channel. The y^*-axis is chosen to go through the middle of the obstruction. The flow is assumed to be uniform far upstream. The dimensionless circle radius

$$\alpha = \frac{R}{H} \tag{2.1}$$

is introduced. The free surface is described by $y^* = H + \eta^*(x^*)$.

The velocity potential satisfies Laplace's equation in the interior of the fluid domain. Bernoulli's equation in the entire fluid takes the form

$$\tfrac{1}{2}\rho(u^{*2} + v^{*2}) + \rho g y^* + p^* = \tfrac{1}{2}\rho U^2 + \rho g H, \tag{2.2}$$

where u^* and v^* are the horizontal and vertical components of velocity, p^* the pressure and ρ the fluid density.

The condition of no flow normal to the bottom $y^* = h^*(x^*)$ may be written

$$u^* h^*_{x^*} = v^* \quad \text{at} \quad y^* = h^*(x^*), \tag{2.3}$$

where

$$h^*(x^*) = \begin{cases} (R^2 - x^{*2})^{\frac{1}{2}} & (|x^*| \leq R), \\ 0 & (|x^*| > R). \end{cases} \tag{2.4}$$

The dynamic condition on the free surface can be written by applying Equation (2.2) on the free surface:

$$\tfrac{1}{2}\rho(u^{*2} + v^{*2}) + \rho g \eta^* = \tfrac{1}{2}\rho U^2. \tag{2.5}$$

3. Weakly nonlinear analysis

One of the main difficulties in computing free-surface flows is to find the number of independent parameters. For that purpose, a weakly nonlinear analysis can be useful.

Let L be the typical wavelength, which is yet to be determined. We use L and the upstream water depth H as the horizontal and vertical scales respectively. The following dimensionless variables are introduced:

$$\begin{aligned} \epsilon &= (H/L)^2 \ll 1 \quad \text{(a small parameter)}, \\ (x, y) &= (\epsilon^{1/2} x^*, y^*)/H, \\ (u, v) &= (u^*, \epsilon^{-1/2} v^*)/\sqrt{gH}, \\ h(x) &= \epsilon^{-2} h^*(x^*)/H \quad \text{(small bump assumption)}. \end{aligned}$$

Let the free-surface elevation and Froude number be described by

$$\frac{\eta^*}{H} = \epsilon\eta, \quad F = 1 + \epsilon\mu. \tag{3.1}$$

The velocity potential is expanded as well in powers of the small parameter ϵ.

After plugging the various expansions into the governing equations and boundary conditions, one obtains a sequence of equations of successive orders. After a few steps, one derives the so-called forced Korteweg–de Vries (fKdV) equation. We believe that the first derivation of the fKdV equation was performed by Akylas [8] (see also Mielke [9] and Kirchgässner [10] for more rigorous derivations). Shen [11, 12] studied the validity of the fKdV equation. The fKdV equation is also given in the monograph by Baines [13, Equation (2.6.2) and the discussion which follows].

Since the present paper deals with stationary solutions, we only write the stationary forced Korteweg–de Vries equation:

$$\tfrac{1}{6}\eta_{xxx} + \tfrac{3}{2}\eta\eta_x - \mu\eta_x = -\tfrac{1}{2}h_x. \tag{3.2}$$

In the absence of forcing, Equation (3.2) reduces to the classical Korteweg–de Vries (KdV) equation. The first integral of Equation (3.2) is

$$\eta_{xx} + \tfrac{9}{2}\eta^2 - 6\mu\eta = -3h, \tag{3.3}$$

under the condition that the flow is uniform far upstream.

For clarity, we also rewrite the fKdV Equation (3.3) in physical coordinates:

$$H^3\eta^*_{x^*x^*} + \tfrac{9}{2}\eta^{*2} - 6H(F-1)\eta^* = -3Hh^*(x^*). \tag{3.4}$$

For obstructions whose height is comparable with the length of the obstruction base ('local' forcing), the forcing can be approximated by the Dirac delta function in the dimensionless long wave coordinates [12]:

$$h(x) = Q\delta(x).$$

In the present study, we consider semi-circular bumps: $y^* = \sqrt{R^2 - x^{*2}}$. In dimensionless coordinates, the semi-circular bump becomes $y = \epsilon^{-\frac{1}{2}}\sqrt{\epsilon\alpha^2 - x^2}$, with support $[-\sqrt{\epsilon}\,\alpha, \sqrt{\epsilon}\,\alpha]$, which is $\sqrt{\epsilon}$ times smaller than the height α. Hence $h(x)$ can be approximated by $Q\delta(x)$. This height α can be viewed as the amplitude of the forcing. Hence $\epsilon^2 = \alpha$, *i.e.*

$$\epsilon = \sqrt{\alpha}. \tag{3.5}$$

Equation (3.5) determines the typical wavelength L. The amplitude Q is determined by the area of the bump:

$$\int_{-\infty}^{\infty} h^*(x^*)\,\mathrm{d}x^* \approx \int_{-\infty}^{\infty} \epsilon^2 H Q\delta(x)\,\mathrm{d}(\epsilon^{-1/2}Hx) = \text{area of the bump}.$$

This leads to

$$Q = (\pi/2)\alpha^{5/4}.$$

Let us now concentrate on solutions of Equation (3.3) with local forcing:

$$\eta_{xx} + \tfrac{9}{2}\eta^2 - 6\mu\eta = -3Q\delta(x). \tag{3.6}$$

In order to study the solutions of the fKdV Equation (3.6), it is convenient to recall first the solutions of the KdV Equation ($Q = 0$). It has two fixed points: $\eta = 0$ and $\eta = \frac{4}{3}\mu$. Integrating the KdV equation once we have

$$\eta_x^2 = 6\mu\eta^2 - 3\eta^3 + \mathcal{C}. \tag{3.7}$$

Solutions of (3.7) depend on the sign of μ. In other words, the solutions depend on whether the flow is subcritical or supercritical.

3.1. Subcritical flow upstream

When the flow is subcritical, $\mu < 0$. The fixed point $\eta = 0$ is a center, while the fixed point $\eta = \frac{4}{3}\mu$ is a saddle point. The phase plane is shown in Figure 2(a). The bounded solutions are either cnoidal waves going around the center, or a solitary wave going to $\eta = \frac{4}{3}\mu$ at infinity. The solitary wave is obtained when $\mathcal{C} = \frac{32}{9}|\mu|^3$ and its profile is given by

$$\eta = \tfrac{4}{3}\mu + \frac{2|\mu|}{\cosh^2\left(x\sqrt{\frac{3}{2}|\mu|}\right)}. \tag{3.8}$$

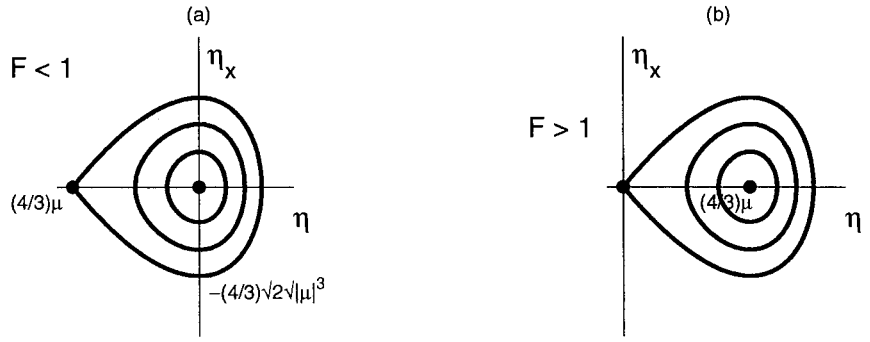

Figure 2. Phase planes corresponding to Equation (3.7) in the unforced case. (a) Subcritical flow ($\mu < 0$). (b) Supercritical flow ($\mu > 0$). The dots represent the fixed points. The outer trajectories are homoclinic solutions, while the inner trajectories are periodic solutions.

In the presence of forcing ($Q \neq 0$), we look for solutions which are continuous and bounded for $x \in \mathbb{R}$, and satisfy

$$\eta_{xx} + \tfrac{9}{2}\eta^2 - 6\mu\eta = 0 \quad \text{for} \quad x \neq 0, \quad \eta_x(0+) - \eta_x(0-) = -3Q.$$

The jump condition is obtained by integrating Equation (3.6) from $0-$ to $0+$.

Since the flow is assumed to be uniform upstream with $\eta = 0$, the solution for $x < 0$ is necessarily $\eta = 0$. At $x = 0+$, the slope of the free surface must be $-3Q$. At the same time, the phase plane shown in Figure 2(a) indicates that the absolute value of the jump of η_x at $\eta = 0$ cannot be greater than $\frac{4}{3}\sqrt{2}|\mu|^{\frac{3}{2}}$. Therefore, for a given upstream Froude number less than unity, there are three possibilities: (i) the obstacle is too large and there is no steady solution, (ii) the obstacle has the size

$$Q_{\max} = \tfrac{4}{9}\sqrt{2}|\mu|^{3/2},$$

which makes the solution jump on the solitary wave solution (3.8) (hydraulic fall), (iii) the amplitude of the forcing is less than $Q_{\max}$ and the solution jumps on a cnoidal wave solution. There is a unique way to perform this jump. When $Q \to 0$, the amplitude of the oscillations tends to zero as well. The solutions are summarized in the (μ, Q)-plane in Figure 3 and corresponding profiles are shown in Figure 4.

3.2. Supercritical flow upstream

When the flow is supercritical, $\mu > 0$. The fixed point $\eta = 0$ is a saddle point, while the fixed point $\eta = \frac{4}{3}\mu$ is a center. The phase plane is shown in Figure 2(b). The bounded solutions are either cnoidal waves going around the center, or a solitary wave going to $\eta = 0$ at infinity. The solitary wave is obtained when $\mathcal{C} = 0$ and its profile is given by

$$\eta = \frac{2\mu}{\cosh^2\left(x\sqrt{\frac{3}{2}\mu}\right)}. \tag{3.9}$$

In the presence of forcing ($Q \neq 0$), we look for solutions which are continuous and bounded for $x \in \mathbb{R}$, and satisfy

$$\eta_{xx} + \tfrac{9}{2}\eta^2 - 6\mu\eta = 0 \quad \text{for} \quad x \neq 0, \quad \eta_x(0+) - \eta_x(0-) = -3Q.$$

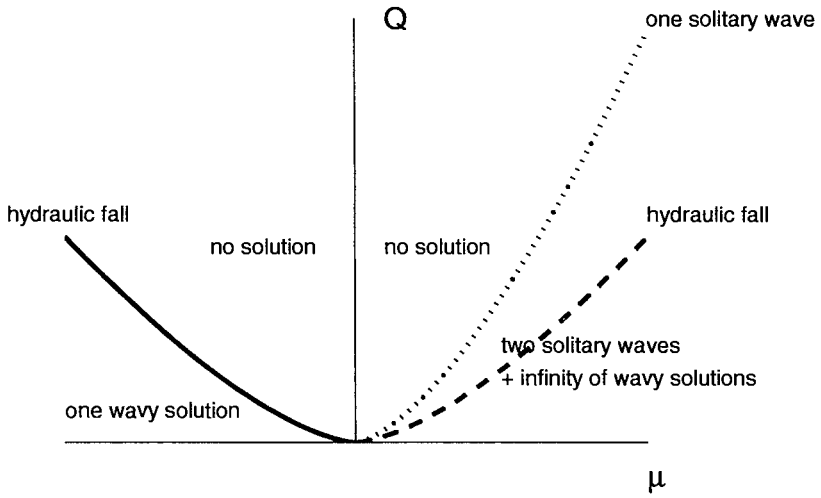

Figure 3. Description of solutions in parameter space. The horizontal axis is the value of the Froude number relative to unity. The vertical axis is the obstacle size. The solid line is given by $Q = \frac{4}{9}\sqrt{2}|\mu|^{3/2}$, the dashed line by $Q = \frac{4}{9}\sqrt{2}\mu^{3/2}$, the dotted line by $Q = \frac{8}{9}\sqrt{2}\mu^{3/2}$.

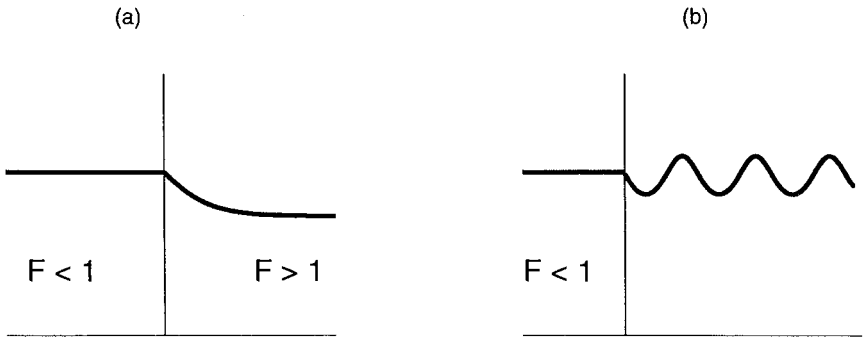

Figure 4. (a) Hydraulic fall with subcritical flow upstream, corresponding to a solution along the solid line in Figure 3. (b) Upstream (subcritical) uniform flow matched with a cnoidal wave downstream. Such a solution lies in the region called 'one wavy solution' in Figure 3.

Since the flow is assumed to be uniform upstream with $\eta = 0$, the solution for $x < 0$ necessarily follows the solitary wave (3.9). At $x = 0$, the jump in the slope of the free surface must be equal to $-3Q$. At the same time, the phase plane shown in Figure 2(b) indicates that the absolute value of the jump cannot be greater than $\frac{8}{3}\sqrt{2}\mu^{\frac{3}{2}}$. There are more possibilities than in the subcritical case: (i) the obstacle is too large and there is no steady solution, (ii) the obstacle has the size

$$Q_{\max} = \tfrac{8}{9}\sqrt{2}\mu^{3/2},$$

which makes the solution jump back on the solitary wave solution (3.9) along $\eta = \frac{4}{3}\mu$ – unique solitary wave, (iii) the amplitude of the forcing is less than $Q_{\max}$ and the solution can either jump back on the solitary wave solution (3.9) (there are two possibilities: one to the left, one to the right of $\eta = \frac{4}{3}\mu$), or jump on a cnoidal wave solution (there are infinitely many possibilities but the wavelength of the cnoidal wave is bounded below). If the obstacle has the

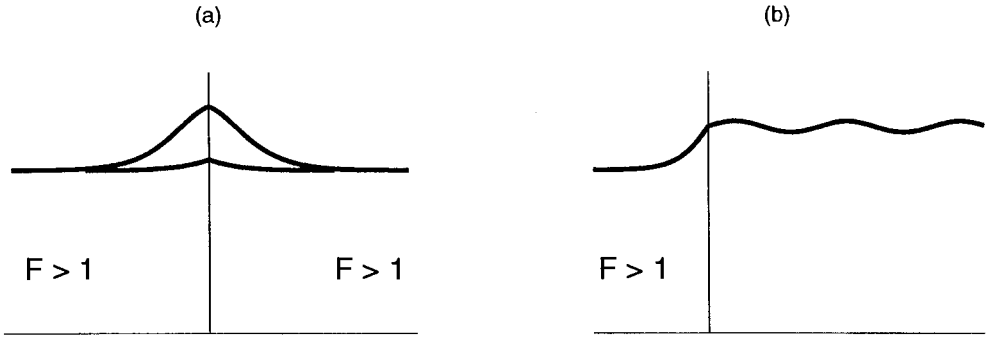

Figure 5. (a) Upstream supercritical flow. The forcing can sustain two symmetric solitary waves. (b) Solution matching the upstream supercritical flow with a cnoidal wave downstream. All these solutions lie in the region called 'two solitary waves + infinity of wavy solutions' in Figure 3.

size

$$Q = \tfrac{4}{9}\sqrt{2}\mu^{3/2} = \tfrac{1}{2}Q_{\max},$$

the wavelength of the cnoidal wave can vanish and one obtains again the hydraulic fall. It is exactly the mirror image of the hydraulic fall obtained in Section 3.1. The solutions are summarized in the (μ, Q)-plane in Figure 3 and corresponding profiles are shown in Figure 5.

The present paper is devoted to the wavy solution. For fixed μ (given Froude number) and Q (given obstruction size), there is a one-parameter family of such solutions. The wavelength is bounded below at some value and can go all the way to infinity to either of the solitary waves. In Section 5, we present numerical evidence of such solutions for the fully nonlinear problem.

4. Numerical scheme

The numerical scheme follows closely that of Forbes and Schwartz [2] and Forbes [4]. We non-dimensionalise the problem by taking U as the unit velocity and H as the unit length. The dimensionless volume discharge is therefore unity. From now on, all the new variables will be dimensionless. For example, x and y will be the dimensionless coordinates. It is convenient at this stage to introduce the complex variable $z = x + \mathrm{i}y$. The z-plane is mapped into a ξ-plane in which the bottom is a straight line by the transformation

$$\xi = \zeta + \mathrm{i}\chi = \frac{1}{2}\left(z + \frac{\alpha^2}{z}\right), \tag{4.1}$$

where α is defined by Equation (2.1). Following [14], we describe the free surface parametrically by $x = X(s)$ and $y = Y(s)$, where s is the arclength. Therefore we require

$$X'^2 + Y'^2 = 1, \tag{4.2}$$

where primes denote derivatives with respect to s. We choose $s = 0$ at the point $x = 0$ on the free surface (*i.e.* $X(0) = 0$). Equation (4.1) can then be used to define the values $\zeta(s)$ and $\chi(s)$ of ζ and χ on the free surface. We also denote by $\phi(s)$ the value of ϕ at a point along the free surface.

Following Forbes and Schwartz [2] and Forbes [4], we derive the integral equation

$$\pi\left[\phi'(s)\frac{\zeta'(s)}{\zeta'^2(s)+\chi'^2(s)} - 2\gamma\right] = \int_{-\infty}^{\infty} \frac{[\phi'(t) - 2\gamma\zeta'(t)][\chi(t) - \chi(s)] + 2\gamma\chi'(t)[\zeta(t) - \zeta(s)]}{[\zeta(t) - \zeta(s)]^2 + [\chi(t) - \chi(s)]^2}\,\mathrm{d}t + \int_{-\infty}^{\infty} \frac{[\phi'(t) - 2\gamma\zeta'(t)][\chi(t) + \chi(s)] + 2\gamma\chi'(t)[\zeta(t) - \zeta(s)]}{[\zeta(t) - \zeta(s)]^2 + [\chi(t) + \chi(s)]^2}\,\mathrm{d}t, \tag{4.3}$$

where the first integral in the right-hand side of (4.3) is a Cauchy principal value. The constant γ is chosen as the undisturbed velocity at $s = -\infty$ (a precise definition is given later).

Next Bernoulli's equation on the free surface yields

$$[\phi'(s)]^2 + \frac{2}{F^2}[Y(s) - 1] = 1. \tag{4.4}$$

This concludes the formulation of the problem as an integro-differential equation. We seek three unknown functions $X(s)$, $Y(s)$ and $\phi'(s)$ satisfying (4.1)–(4.4). We solve this equation numerically by introducing the mesh points

$$s_I = -\frac{(N-1)E}{2} + (I-1)E, \qquad I = 1, \ldots, N, \tag{4.5}$$

the midpoints

$$s_I^M = \frac{s_I + s_{I+1}}{2}, \qquad I = 1, \ldots, N-1, \tag{4.6}$$

and the unknowns $X_I' = X'(s_I)$, $Y_I' = Y'(s_I)$ and $\phi_I' = \phi'(s_I)$, $I = 1, \ldots, N$.

We satisfy (4.2) and (4.4) at the mesh points s_I and (4.3) at the mesh points s_I^M. This leads to $3N - 1$ equations. Details on the finite-difference formulas used can be found in Forbes [4] and Forbes and Schwartz [2]. One more equation is obtained by using Bernoulli's equation to define the undisturbed depth as $s \to -\infty$ by

$$\gamma^2 + \frac{2}{\gamma F^2} - 1 - \frac{2}{F^2} = 0. \tag{4.7}$$

For given values of α and F, we now have $3N$ equations for the $3N + 1$ unknowns X_I', Y_I', ϕ_I' and γ. The last equation is obtained by fixing a third parameter. We found it convenient to choose this parameter as the value of Y_1. Therefore the last equation is

$$Y_1 = \delta, \tag{4.8}$$

where δ is given. This system of $3N + 1$ algebraic equations with $3N + 1$ unknowns is solved by Newton iterations. We note that the parameter δ has no physical meaning. Our approach can be viewed as an inverse approach. We compute solutions for given values of α, F and δ. Once a solution has been obtained, it can be interpreted as a solution characterised by given values of α, F and a third parameter such as the wavelength or amplitude of the downstream waves.

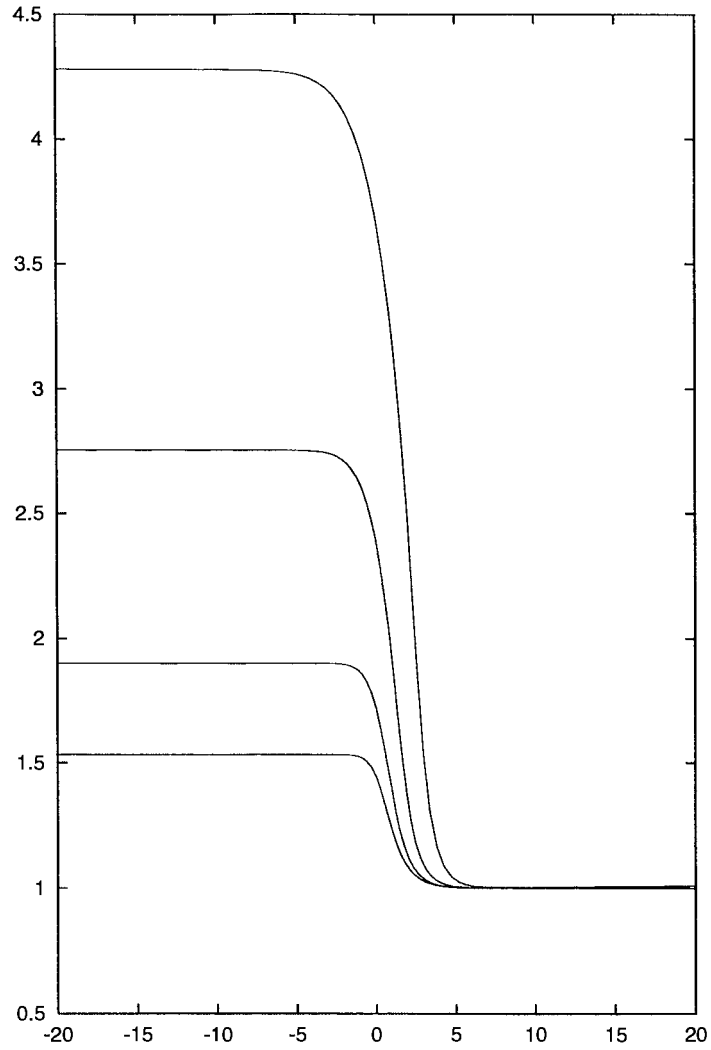

Figure 6. Hydraulic falls for various values of α. The flow is subcritical on the left and supercritical on the right. The profiles from bottom to top correspond to $\alpha = 0{\cdot}3$, $0{\cdot}5$, $1{\cdot}0$ and $2{\cdot}0$. The corresponding Froude numbers are $F = 1{\cdot}36$, $1{\cdot}58$, $2{\cdot}01$ and $2{\cdot}63$.

5. Numerical results

The numerical scheme described in Section 4 was used to calculate solutions for various values of α, $F > 1$ and δ. Most results presented were obtained with $N = 130$. We repeated some of the calculations with $N = 260$ to check that the results presented are correct within graphical accuracy.

Our numerical results agree with the weakly nonlinear theory of Section 3.2 in the sense that there is a one-parameter family of waveless solutions (hydraulic fall) and a three-parameter family of solutions with waves as $s \to -\infty$. The three parameters are here chosen as α, F and δ. These solutions lie in the region called 'two solitary waves + infinity of wavy solutions' in Figure 3. The computations were focused to a neighborhood of the dashed line 'hydraulic fall.'

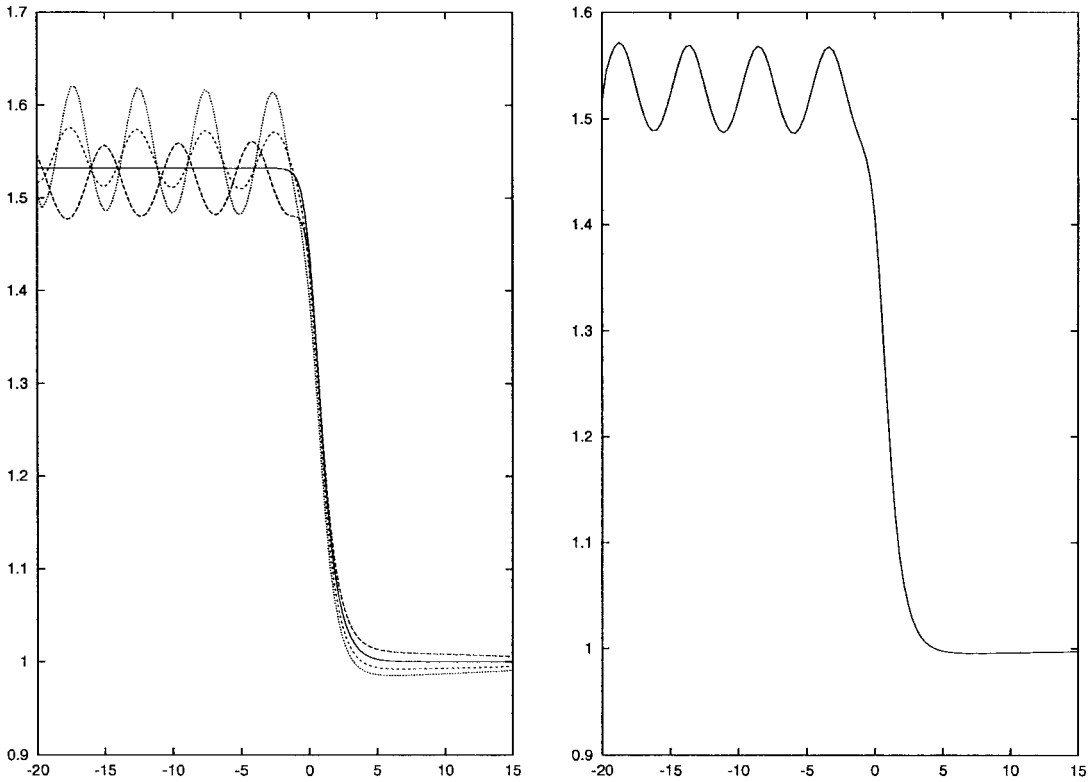

Figure 7. (a) Computed free surface profiles for $\alpha = 0{\cdot}3$ and $F = 1{\cdot}36$. The solid curve is a waveless solution. (b) A typical free-surface profile corresponding to a member of the one-parameter family of solutions for $\alpha = 0{\cdot}3$ and $F = 1{\cdot}355$.

The one-parameter family of waveless solutions is a sub-family of the three-parameter family. We can compute it directly by modifying the scheme of Section 4 by allowing F and δ to be unknowns. We then need two extra equations. These are obtained by forcing the free surface to be without waves as $s \to -\infty$ with the two conditions

$$Y_1' = Y_2' = 0. \tag{5.1}$$

The parameter is then α. Typical hydraulic falls are shown in Figure 6. Note that the uniform flow with constant velocity U and constant depth H is on the far left in Figure 5(b) and on the far right in the numerical results. These solutions were found to be in close agreement with the solutions previously computed by Forbes [4]. As $\alpha \to 0$, $F \to 1$ and the flow reduces to a uniform stream. Solutions exist for arbitrary large values of α. We note that solutions similar to those in Figure 6 were obtained by a different numerical method for triangular obstacles (Dias and Vanden-Broeck [5]).

Particular members of the three-parameter family of solutions are shown in Figure 7(a). For $\alpha = 0{\cdot}3$, the waveless solution of Figure 6 corresponds to $F = 1{\cdot}36$. The profiles of Figure 7(a) are for these values of α and F and various values of δ. The results show that we recover the hydraulic fall for a particular value of δ. Of course if we fix $\alpha = 0{\cdot}3$ and a value of $F \neq 1{\cdot}36$, we do not recover the hydraulic fall by varying δ. All the profiles have then waves downstream. This is illustrated in Figure 7(b), where we show a free-surface profile for $\alpha = 0{\cdot}3$, $F = 1{\cdot}355$.

Finally let us mention that the solutions in Figure 7 will only satisfy the radiation condition if the flows are from the right to the left. On the other hand no radiation condition needs to be satisfied for the hydraulic falls of Figure 6 and the flow can be either to the right or to the left since potential flows are reversible.

6. Conclusion

We have considered steady nonlinear free surface flows past a submerged obstacle. Both weakly nonlinear and fully nonlinear solutions were presented. The weakly nonlinear theory enabled a systematic investigation of the various types of solutions and of the corresponding numbers of independent parameters. Previous calculations by [2], [4], [5] and others have provided fully nonlinear numerical solutions for all the types of solutions predicted by the weakly nonlinear theory except one. The numerical computations described in Sections 4 and 5 provide solutions for this previously missing type of fully nonlinear solutions.

Acknowledgements

This work was supported in part by EPSRC and the Leverhulme Trust. Part of this work was performed at the Isaac Newton Institute for Mathematical Sciences, University of Cambridge, during the programme on Surface Water Waves which was held in August 2001.

References

1. H. Lamb, *Hydrodynamics*, 6th ed. Cambridge University Press (1932) 738 pp.
2. L.K. Forbes and L.W. Schwartz, Free-surface flow over a semicircular obstruction. *J. Fluid Mech.* 114 (1982) 299–314.
3. J.-M. Vanden-Broeck, Free-surface flow over a semi-circular obstruction in a channel. *Phys. Fluids* 30 (1988) 2315–2317.
4. L.K. Forbes, Critical free-surface flow over a semi-circular obstruction. *J. Eng. Math.* 22 (1988) 3–13.
5. F. Dias and J.-M. Vanden-Broeck, Open channel flows with submerged obstructions. *J. Fluid Mech.* 206 (1989) 155–170.
6. R. H. J. Grimshaw and N. Smyth, Resonant flow of a stratified fluid over topography. *J. Fluid Mech.* 169 (1986) 429–464.
7. P. Milewski and J.-M. Vanden-Broeck, Time dependent gravity–capillary flows past an obstacle. *Wave Motion* 29 (1999) 63–79.
8. T.R. Akylas, On the excitation of long nonlinear water waves by a moving pressure distribution. *J. Fluid Mech.* 141 (1984) 455–466.
9. A. Mielke, Steady flows of inviscid fluids under localized perturbations. *J. Diff. Eqs.* 65 (1986) 89–116.
10. K. Kirchgässner, Nonlinearly resonant surface waves and homoclinic bifurcation. *Adv. Applied Mech.* 26 (1988) 135–181.
11. S.S.-P. Shen, Forced solitary waves and hydraulic falls in two-layer flows. *J. Fluid Mech.* 234 (1992) 583–612.
12. S.S.-P. Shen, On the accuracy of the stationary forced Korteweg–de Vries equation as a model equation for flows over a bump. *Q. Appl. Math.* 53 (1995) 701–719.
13. P.G. Baines, *Topographic effects in stratified flows.* Cambridge University Press (1995) 482 pp.
14. L.K. Forbes, Two–layer critical flow over a semi–circular obstruction. *J. Eng. Math.* 23 (1989) 325–342.